The oceanic budgets of nickel and zinc isotopes: the importance of sulphidic environments as illustrated by the Black Sea

Derek Vance[1*], Susan H. Little[1,2], Corey Archer[1], Vyllinniskii Cameron[3], Morten Andersen[1,4], Micha J.A. Rijkenberg[5] and Timothy W. Lyons[6]

[1]Institute of Geochemistry and Petrology, Department of Earth Sciences, ETH Zürich, Clausiusstrasse 25, 8092 Zürich, Switzerland.

[2] Department of Earth Science and Engineering, Imperial College London, London SW7 2BP, UK.

[3]Department of Earth Sciences, University of Bristol, Wills Memorial Building, Queens Road, Bristol BS8 1RJ, UK.

[4]School of Earth & Ocean Sciences, Cardiff University, Cardiff CF10 3AT, UK

[5] NIOZ Royal Netherlands Institute for Sea Research, Department of Ocean Systems (OCS), and Utrecht University, P.O. Box 59, 1790 AB Den Burg, Texel, The Netherlands.

[6] Department of Earth Sciences, University of California, Riverside, California, 92521, USA.

* Corresponding author: derek.vance@erdw.ethz.ch.

2 tables.
7 figures.
8900 words.

Summary

Isotopic data collected to date as part of the GEOTRACES and other programmes show that the oceanic dissolved pool is isotopically heavy relative to the inputs for zinc (Zn) and nickel (Ni). All Zn sinks measured until recently, and the only output yet measured for Ni, are isotopically heavier than the dissolved pool. This would require either a non-steady state ocean or other unidentified sinks. Recently, isotopically light Zn has been measured in organic carbon-rich sediments from productive upwelling margins, providing a potential resolution of this issue, at least for Zn. However, the origin of the isotopically light sedimentary Zn signal is uncertain. Cellular uptake of isotopically light Zn followed by transfer to sediment does not appear to be a quantitatively important process. Here, we present Zn and Ni isotope data for the water column and sediments of the Black Sea. These data demonstrate that isotopically light Zn and Ni are extracted from the water column, likely through an equilibrium fractionation between different dissolved species followed by sequestration of light Zn and Ni in sulphide species to particulates and the sediment. We suggest that a similar, non-quanitative, process, operating in porewaters, explains the Zn data from organic carbon-rich sediments.

Keywords: Zinc, nickel, isotopes, Black Sea, oceanic budgets, GEOTRACES.

Introduction

The GEOTRACES programme has added new impetus to the long-standing interest in the geochemistry of the transition metals in the oceans [e.g. 1,2]. As a result of relatively recent advances in our ability to analyse them [e.g. 3-6], the stable isotope systems of these elements have become part of the toolbox available to chemical oceanographers in the pursuit of this interest. Thus, in the past few years, full depth profiles, and even the first oceanic sections, of the stable isotopes of copper [7-9], iron [e.g. 10,11], cadmium [12-16], zinc [16-18], and nickel [19] have become available. These data and their interpretation have been the focus of two broad scientific questions, each with potential applications in Earth history.

The first of these questions has emphasised the potential of the stable isotope systems to contribute to our understanding of transition metals as micronutrients. Transition metals are essential components of enzymes and proteins, and may be close to limiting to phytoplankton in the photic zone of the world's oceans [e.g. 20]. Consistent with this role, they often show nutrient-like depth profiles in the open ocean, with depletion factors of up to several hundred in the sunlit upper ocean relative to the highest concentrations in the deep. It seems highly likely that biology plays a prominent role in the extreme drawdown of metals like Cd and Zn in the photic zone. If so, and to the extent that biological uptake is associated with an isotope fractionation [e.g. 21-23], there is potentially a great deal to be learnt from these isotope systems about the controls on this important oceanic process. In an Earth Science context, one medium-term objective is the study of past oceanic trace metal distributions and their potential impact on the dynamics of the biological pump, as first envisaged by Martin [2].

Secondly, the budgets of transition metals and their isotopes in the ocean as a whole can set constraints on the relative size and importance of sources and sinks on timescales of the order of their oceanic residence time or longer. It is this latter topic, in particular with respect to the isotope systems of Zn and Ni, that is our focus in this paper. By analogy with molybdenum and uranium [e.g. 24-29], investigations of secular change in the oceanic mass balance of Zn and Ni isotopes hold real potential for understanding past variations in the size of oceanic inputs, such as chemical weathering of the continents, and outputs from the ocean to sediment. By contrast with Mo and U, which behave conservatively in the modern ocean, such studies may potentially be complicated by heterogeneity in the isotopic composition of the dissolved marine pool driven by internal biogeochemical cycling. Such applications to Earth history have barely begun for these isotope systems [e.g. 30,31] and are still dependent on progress in understanding the modern cycles.

Little et al. [32] compiled isotopic data for the known oceanic inputs and outputs of both Zn and Cu in the first comprehensive assessment of the overall oceanic isotopic cycles for these elements. The main conclusion of that study, modified slightly based on more recent findings in this very fast-moving field, is illustrated in Fig. 1. The repeated finding to date in studies of the Zn isotope composition of the dissolved pool, representing nearly 700 isotope analyses from the Pacific, Atlantic and Southern Oceans, is that the sub-thermocline ocean is extremely homogeneous. Excluding data that have been specifically identified by the authors [16,18] as impacted by local hydrothermal and benthic sources, nearly 300 analyses of this dominant deep ocean pool give a $\delta^{66}Zn = +0.51 \pm 0.14$ ($\delta^{66}Zn$ = parts per thousand deviation of the $^{66}Zn/^{64}Zn$ ratio from the Lyon JMC standard, mean and 2SD). The inputs to the ocean identified so far are lighter than this (Fig. 1). Specifically, Little et al. [32] presented data for the dissolved pool of large world rivers and oceanic aerosols, both with abundance-weighted $\delta^{66}Zn \sim +0.3‰$. In this light, the observation that the outputs to sediment [32] are distinctly heavier than the deep ocean dissolved pool can only mean one of two things: either the oceans are not in steady-state with respect to the inputs and outputs, or there are sources and sinks that are missing from their analysis. The available data for the temporal evolution of the oceanic dissolved pool of Zn isotopes [32] present no evidence for non-steady-state behaviour.

Recent data compound the problem. Since the study of Little et al. [32], Conway and John [16,18] documented local enrichments in dissolved Zn near mid-ocean ridges and close to the sediment-water interface along ocean margins. Though the authors noted the very local impact of these hydrothermal and benthic sources, the enrichments are accompanied by locally light Zn isotopes. Thus, though these sources at present appear to be small, they worsen the problem of the oceanic mass balance. More recently, Little et al.

[38] provided a potential solution to the isotopic imbalance by measuring the isotopic composition of Zn in organic-rich sediments along the productive upwelling margin of the Americas, which they found to be lighter than the inputs. Using Zn-Al systematics to separate the authigenic and detrital pool, they estimated the isotopic composition of the authigenic Zn pool to be dominantly between about -0.4‰ and +0.1‰. Though Little et al. [32] estimated the relative sizes of the sinks and sources of Zn to the dissolved pool of the oceans, they acknowledged that these estimates are uncertain, often derived by tying the fluxes of Zn to better known but also imprecise estimates of fluxes of other elements such as Si, Ca and Mo. The implication of the isotopic data in Fig. 1 is that, regardless of the absolute sizes of the various sources and sinks, isotopically light organic-rich sediments must dominate the oceanic output if the oceans are to be in steady-state.

We know much less about the Ni isotope balance in the oceans, but what we *do* know is also summarised in Fig. 1, and it is already clear that there are also budgetary problems. For Ni the stable isotope system of the dissolved pool has been the subject of only one study, which again covers the Pacific, Atlantic and Southern Oceans [19]. As for Zn, that study showed that the riverine and dust inputs to the oceans were distinctly lighter than the oceanic dissolved pool. Although the Ni isotopic composition of Fe-Mn crusts [37], a proxy for the output of Ni to sediment via scavenging to Fe-Mn oxide particulates, is highly variable, the average is very close to the oceanic dissolved pool and probably slightly heavier. Once again, and independent of any imprecision in the estimates of absolute sizes of the sources and sinks, there is a requirement for an isotopically light sedimentary output.

Clearly, the output of isotopically light Zn to organic carbon-rich sediments is critical to the oceanic mass balance of Zn isotopes, but the controls on this important output are unknown. One obvious possibility is that phytoplankton take up light Zn in the photic zone and that the portion that survives bacterial respiration in the deep ocean is transferred to sediment. Globally, diatoms are by far the most important exporters of photosynthetically fixed organic carbon from the surface ocean [e.g. 39]. Given that the organic portions of diatom cells contain up to about 15 times more Zn than average oceanic phytoplankton [e.g. 40], they must completely dominate Zn export. However, there is increasing evidence that uptake of Zn into diatoms does not fractionate Zn isotopes. For example, across a close to two-orders-of-magnitude drawdown in dissolved Zn concentrations in the Atlantic sector of the Southern Ocean, as water is first upwelled and then moved northward at the surface, Zn isotopes in the residual dissolved pool do not change beyond analytical uncertainty [17, 41], implying no fractionation of Zn isotopes upon cellular uptake. Though this finding does not rule out the uptake of isotopically light Zn into cells in different ecological regimes, the dominance of (high Zn) diatoms suggests that these other organisms may not be quantitatively important in export from the upper ocean and output to sediment. A second possibility is that a process within the sediment partitions isotopically unfractionated Zn, delivered to the sediment with organic carbon, into an isotopically light pool that is retained in sediment and a heavy pool that is returned to the oceanic dissolved pool. One obvious possibility for such a process is the sequestration of light Zn isotopes from pore waters into metal sulphide mineral phases, and diffusion of the heavy Zn back out of the sediment into the ocean bottom.

Our purpose in this contribution is to shed light on the potential impact of this process. To this end, we present data that document the behaviour of both Zn and Ni isotopes in the Black Sea, whose deep water column is sulphidic, in order to isolate the impact of sulphidisation of Zn (and Ni) from that of biological uptake. The data highlight the importance of sulphide species of both Zn and Ni in the water column and the delivery of these species from the dissolved pool to sediment. In a set of processes that recall those that control Mo and U, we illustrate the likelihood that it is the sulphidisation of Ni and Zn that exerts an important, likely key, control on oceanic Zn and Ni isotopes.

Samples

The Black Sea is the world's largest permanently anoxic basin, with anoxia driven by restricted water exchange with the Mediterranean Sea, strong vertical stratification across the permanent halocline and moderate primary productivity. This vertical stratification limits the supply of oxygen to the deep basin, leading to the development of sulphidic conditions due to the respiration of organic carbon [e.g. 42]. As a result, the complete redox gradient observed during oxidation of organic matter in sediments worldwide,

from oxic to suboxic to anoxic and ultimately sulphidic waters, can be sampled in the top 150m or so of the water column. Similarly, cores recovered from depth transects in the Black Sea record redox conditions in the overlying water column that range from oxic on the shallow shelf to anoxic and sulphidic in the deep basin [e.g. 43,44]. The depth of the oxic-anoxic transition varies from around 100m in the central parts of the basin, from which our water column samples derive, to about 150m near the margins [e.g. 45].

Seawater

Black Sea water column samples were collected during leg 2 of the MedBlack GEOTRACES cruise (64PE373) on the *RV Pelagia*, 13-25 July 2013 (Fig. 2). A total of 12 full depth profile stations were sampled on this cruise. Of these, large volume samples were collected for metal stable isotope analysis at two hyper stations – Stations 2 and 5 – for which data are presented here. The two depth profiles sampled the well-known redox structure of the Black Sea [e.g. 46] including an oxic surface layer above the permanent halocline and down to about 70m, a sub-oxic zone, and a permanently anoxic and sulphidic deep layer beneath about 100m (Fig. 3). Samples for this study were collected using an ultra-clean all-titanium frame with 24 sample bottles of 27 L each made of PVDF plastic and deployed on a Kevlar hydrowire [47]. Samples were filtered on board in a class 100 clean container under nitrogen pressure using 0.2 μm Sartobran 300 cartridges into pre-cleaned LDPE bottles and acidified to pH ~2 using ultrapure SEASTAR HCl.

Sediments

The samples analyzed in this study for Ni and Zn isotopes come from four sites (Fig. 2), for which an extensive dataset for redox-sensitive trace metal concentrations has recently been reported [48]. Two basinal sites, stations 9 and 14, underlie the strongly euxinic part of the water column. Organic carbon contents at these two stations are about 5 weight percent [44]. Station 16 is from the oxic shelf margin, with a predominantly detrital influence, while station 16B is also oxic but from close to the modern-day chemocline. Lyons [43] provides additional details regarding the sedimentological characteristics of these samples. In addition, the euxinic samples have been studied previously for their carbon-sulfur-iron systematics [44], sulfur isotope trends [49], Fe isotopes [50], Mo concentrations and isotopes [24,51] and uranium concentrations and isotopes [26]. The samples from stations 16 and 16B have been the subject of a chemocline study in Lyons et al. [52]. Further geochemical data for all four stations can be found in Lyons and Severmann [53]. Concentrations of Ni, Zn and Al presented in Table 1 here are taken from Little et al. [48].

River Danube

The Danube sample was collected in August 2014, just upstream of the town of Tulcea, Romania, around 50km upstream from the outlet to the Black Sea. The sample was collected from mid-stream into a pre-cleaned LDPE bottle, filtered to 0.45μm just after collection and acidified to pH 2 on return to the laboratory in Switzerland.

Methods

Our methods for most aspects of the Zn and Ni isotopic analysis of seawater, river waters and sediments have been published previously. Where this is the case, only a brief summary is given here. For some of the Black Sea water column samples we have used a pre-concentration approach that is new to our group, and this is explained in more detail below. All water samples were spiked with both ^{67}Zn-^{64}Zn and ^{61}Ni-^{62}Ni double spikes before any of the chemical treatments described below. Sediment samples were spiked once in solution in HCl. Our methods for the use of the double spike approach to the correction of artefactual mass discrimination have been described in detail in previous papers [3,17,19,54].

When this study began we were using the same pre-concentration approach for seawater samples that we have described in earlier papers [17,19]: the addition of a small amount of Al to spiked and acidified

seawater samples followed by co-precipitation of the metals of interest with $Al(OH)_3$ by raising the pH to about 8.5. Ni isotope data for Station 2 were produced using this approach. Later in the study a new procedure was introduced and was used to produce the Ni data for Station 5 and all the Zn data. Metals were pre-concentrated from up to 2L of seawater using an ethylenediaminetriacetic acid chelating resin, sold commercially as Nobias PA-1 (Hitachi Technologies: [5,55]). Nobias resin was held in PFA Teflon cartridges, with a resin bed of 12mm diameter by 40 mm length. Samples were loaded onto the columns using a peristaltic pump, and trace metals were eluted using nitrogen gas pressure and a flow-through procedure modified from Takano et al [5]. Prior to pre-concentration, pH 2 acidified samples were equilibrated for 24 hours with Ni and Zn double spikes. Samples were then adjusted to pH 5±0.3 using an ammonium acetate buffer, made to a final acetic acid concentration of 30mM, before loading onto the column. Matrix cations, principally Na and Mg, were eluted with 200ml of 30 mM ammonium acetate buffer, followed by the elution of the trace metal budget using 20 ml 1M HNO_3.

The Danube river sample was pre-concentrated by drying down, followed by treatment with concentrated nitric acid to digest residual organics and final dissolution in 7M HCl. The sediment samples (50-100 mg) were first treated with dilute nitric acid to dissolve carbonate, and then digested in a 3:1 mix of concentrated HF and HNO_3. This was followed by three treatments with concentrated nitric acid to dissolve residual fluoride salts before final dissolution in 7M HCl.

To separate individual transition metals from each other and from the matrix, the dissolved bulk sediment or the pre-concentrated water samples were first passed through an anion-exchange column (Bio-Rad AG MP-1M resin) using procedures described in detail previously [56]. This produces an impure Ni fraction and a relatively pure Zn fraction. This Zn fraction was further purified by a second pass through this anion column. The impure Ni fraction was passed through a DMG column and a further small anion column (to remove any residual Fe), as described in Cameron et al. [54] and Cameron and Vance [19]. Isotopic analyses were performed using a Thermo-Finnigan Neptune multi-collector inductively-coupled-plasma mass spectrometer (MC-ICP-MS) at the University of Bristol (Black Sea sediments) or a Thermo-Finnigan NeptunePlus at ETH Zürich (all water samples). Zinc and nickel were introduced into the mass spectrometer in 0.3M nitric acid via a CPI PFA nebuliser (50µl/minute) or a Savillex C-Flow PFA nebuliser (50µl/minute) attached to an Aridus. The analysis consumed approximately 30 ng of Zn or Ni. For Zn analyses, ^{62}Ni was measured to monitor a potential interference on ^{64}Zn from ^{64}Ni, and mass 68.5 measured to monitor potential interferences from doubly-charged Ba species on Zn isotopes. For Ni, ^{56}Fe was measured as a monitor of a potential interference from ^{58}Fe on ^{58}Ni. In all cases these measured interferences were negligible. Mass discrimination was corrected using the double spike, as detailed previously [3,17,19,54]. All the double spikes in our laboratory are cleaned of other elements before use, by passage through equivalent columns to those we use for samples, and to allow spiking of the same sample for multiple elements despite the fact that e.g. the (uncleaned) Zn spike contains small amounts of Ni impurity etc. All Ni and Zn isotopic compositions are given in standard notation as follows relative to the NIST SRM986 and JMC Lyon Zn standards respectively:

$$\delta^{66}\mathrm{Zn} = 1000\left[\frac{\left(^{66}\mathrm{Zn}/^{64}\mathrm{Zn}\right)_{\mathrm{sample}}}{\left(^{66}\mathrm{Zn}/^{64}\mathrm{Zn}\right)_{\mathrm{Lyon\ JMC}}} - 1\right]$$

$$\delta^{60}\mathrm{Ni} = 1000\left[\frac{\left(^{60}\mathrm{Ni}/^{58}\mathrm{Ni}\right)_{\mathrm{sample}}}{\left(^{60}\mathrm{Ni}/^{58}\mathrm{Ni}\right)_{\mathrm{NIST\ SRM986}}} - 1\right]$$

Long-term reproducibility of isotopic analyses was ±0.06‰ for both isotope systems. This was assessed over the course of this and parallel studies, through repeat measurements of primary JMC and NIST standards as well as a secondary standard each for Zn (IRMM-3702) and Ni (USGS Fe-Mn nodule, Nod-P1, digested and passed through the Ni column chemistry). These latter give $\delta^{66}Zn_{JMC\text{-}Lyons}$ = +0.30±0.06 (2 SD, n =163 over 24 months) and $\delta^{60}Ni_{NIST\ SRM986}$ = +0.33±0.06 (2SD, n = 17 over 8 months). Internal errors obtained from the mass spectrometric analysis and propagated through the double spike algebra were virtually always substantially lower than long-term reproducibility, and it is the latter that is given as the uncertainty in the tables in this paper, except for the occasional analysis where internal errors are indeed higher. Procedural blanks for sediment samples, for the Danube River sample, and for the seawater samples pre-concentrated with Nobias were 0.2-3% of the analysed sample size, so that corrections to the measured isotopic compositions would be negligible and have not been applied. For the seawater samples whose Ni isotopic compositions were measured following pre-concentration by Al co-precipitation (Station 2), the measured total blank is 23±0.8 ng (n = 8) and has a δ^{60}Ni = +0.04±0.09‰. Such a blank would imply corrections to sample isotopic compositions that are about the same as the reproducibility quoted above – in other words also barely significant – and have not been applied here.

Results

Water samples

Chemical and isotopic data for the Black Sea water column and the River Danube are presented in Table 1 and as depth profiles in Fig. 3. The upper 300m of the water column show essentially identical features at the two stations, for Zn and Ni concentrations as well as their isotope systems. Note that the Ni data for the two stations were obtained using two different pre-concentration methods.

Our concentration data for both Zn and Ni at both stations show a very similar pattern to a previously published profile from the northwestern Black Sea [57]. The Zn concentration profile can be conveniently separated by the concentration maximum at about 70m (4.95 nmol kg^{-1}, 69m, Station 2), from which concentrations decline towards the surface (0.7±0.1 nmol kg^{-1} at 10m) and into the deep sulphidic portion of the water column (minimum of 0.26-0.31 nmol kg^{-1} at depth 300m). The decline towards the surface is very well correlated with Si (Fig. 4) and seems likely to be driven by phytoplankton uptake. δ^{66}Zn is homogeneous at 70m and shallower at both stations, at +0.23±0.05‰, despite the surface-ward drop in concentrations. However, there is a dramatic shift towards isotopically heavy Zn beneath 70m, reaching a maximum δ^{66}Zn of around +1.23±0.03‰ at both stations at about 150m (where Zn concentrations are still 2-3 times higher than the water column minimum). Between 150m and the concentration minimum at 300m δ^{66}Zn declines very slightly to +1.09‰ at both stations. The isotope profiles at the two stations diverge in the bottom 1 km of the water column. δ^{66}Zn at Station 5 remains heavy all the way down to the bottom, at +1.17±0.07‰, and concentrations remain very low, at between 0.31 and 0.43 nmol kg^{-1}. At Station 2, on the other hand, our first analysis yielded anomalous data whereby δ^{66}Zn shifts back to light values downward, reaching +0.36‰ at 2070m before kicking back to +0.8‰ again in the bottom-most sample. Accompanying this isotopic shift, concentrations are elevated by up to factor 2.5 relative to equivalent depths at Station 5 (Table 1). We suspected that this difference between the two stations, given the near identity of the rest of the Ni and Zn concentration and isotope profiles, was due to contaminated bottles at Station 2. We have analysed Zn and its isotopes from a second bottle for three of these depths, and these second analyses yielded data much more in line with the rest of the profiles. Both analyses are shown in Table 1, with the anomalous data given in bold italics. These data are excluded from further discussion below.

Nickel concentrations vary much more subtly in the Black Sea water column than those of Zn, but the small variation (10-13 nmol kg^{-1}) is very coherent between the two stations, and there is a very tight anti-correlation with δ^{60}Ni for most of the water column (Fig. 3). Unlike Zn, Ni is not drawn down in the photic zone, and the upper 80m shows [Ni] = 11.3±0.4 nmol kg^{-1}. Despite this homogeneity, there is a distinct maximum in δ^{60}Ni at 70-80m (δ^{60}Ni = +1.47±0.04‰ relative to +1.18±0.02 at 9-10m) in the suboxic zone, just above the rise in sulphide concentrations beneath about 100m (Fig. 3). The initial rise in sulphide beneath 100m is accompanied by a peak in Ni concentrations (13 nmol kg^{-1} centred on 130m). This peak is

coincident with a prominent minimum in δ^{60}Ni (at +0.79±0.04‰). Concentrations decline again, and δ^{60}Ni increases to another more subtle reversal at about 300m ([Ni] = 10 nmol kg^{-1}, (δ^{60}Ni = +2.01±0.04‰). In the bottom km of the water column, Ni concentrations rise again to 12 nmol kg^{-1}, while δ^{60}Ni declines very slightly to +1.9±0.1‰.

The Ni isotopic composition of the River Danube is very close to the surface Black Sea samples at δ^{60}Ni = +1.25‰, with concentrations about 50% higher at 18 nM kg^{-1}. Zinc concentrations in the Danube are a bit more than double the maximum seen in the Black Sea water column, at around 11 nmol kg^{-1}, and have an extremely light isotopic composition, with a δ^{66}Zn value of about -0.8‰. Though the Zn concentration is within the range measured in relatively undisturbed catchments such as the Amazon and the Kalix (Arctic Circle, Northern Sweden), the isotopic composition is much lighter than anything yet measured in the still small Zn isotope dataset for relatively uncontaminated world rivers [32]. It is worth noting, however, that δ^{66}Zn values as low as -0.6 have recently been measured in the Rio Grande system [58], where isotopically light Zn is derived from acidic drainage of hydrothermal deposits and is further fractionated as sorption at higher pH removes heavy Zn to particulates. It is also worth noting that, including the Danube analysis, the total range of Zn isotope compositions measured in water from the Black Sea system is 2.1‰, versus the total published range for rivers and the entire open ocean of 2.25‰ (Fig. 1).

Sediment

Sediment data are presented in Table 2 and are shown on isotope versus metal/Al plots in Figure 5. Zinc concentrations range from 16 to 104 ppm while δ^{66}Zn varies from +0.23 to +0.56‰. As noted by Little et al. [48], following many previous workers, authigenic metal enrichments in sediments are often identified using metal/Al ratios, the rationale being that excess Zn over the detrital pool will be accompanied by little or no Al. Zinc enrichments in sediments are more difficult to spot than for some elements – such as Mo - simply because the detrital background Zn concentration can be on the order of 10-100 ppm, compared to ~ 1 ppm for Mo. Nonetheless, the two-to-nine-times higher Zn/Al ratios in euxinic compared to oxic Black Sea sediments (Fig. 5a) imply *absolute amounts* of authigenic Zn of 10-80μg per gram of sediment (or 65±25% of the total sediment inventory), comparable with those of Mo (18-51 μg/g; [48]). Fig 5a suggests that Zn isotopes in euxinic Black Sea sediments are adequately explained by two component mixing between a detrital pool that dominates sediments recovered from the oxic shelf, with a δ^{66}Zn around +0.25 to +0.30‰ and a Al/Zn ratio around 0.1x10^{-4}, and an authigenic Zn pool at Al/Zn = 0 and with a δ^{66}Zn around +0.5 to +0.6‰.

Nickel concentrations in Black Sea sediments are 21-93 ppm, and δ^{60}Ni ranges from +0.14 to +0.51‰. The sediments also show authigenic enrichments in Ni, though these are more subtle than for Zn (Fig. 5b). Ni/Al ratios in the euxinic sediments are up to factor of about three higher than in sediments from the oxic shelf, suggesting that, on average, around half the Ni (or ~20 μg/g) in the sediment is authigenic. The plot of the isotopic composition is also more ambiguous for Ni than for Zn. The majority of data imply an authigenic δ^{60}Ni (Al/Ni = 0) of around +0.3‰, while a few outliers may hint at a second trend pointing to a value more like +0.6‰.

Discussion

Zn and its isotopes in the oxic regime: lack of biological fractionation

As noted earlier, the Zn concentration maximum at around 70m clearly splits the Black Sea water column into two regimes. From 70m upwards, Zn concentrations decrease by close to an order of magnitude (from 5 to 0.6 nmol kg^{-1} at Station 2 where the higher resolution depth profile best captures the maximum) while δ^{66}Zn does not change outside of analytical uncertainty, remaining at +0.23±0.05‰. From 70m downwards concentrations also decrease, this time by slightly more than an order of magnitude (from 5 to 0.3nmol kg^{-1}), but in this case δ^{66}Zn shifts to dramatically heavier values, to +1.23±0.03‰ at 150m. In these first two sections of the discussion we will treat these two different regimes separately.

The drop in Zn concentrations towards the surface in the upper 70m of the water column is well correlated with the major nutrients, particularly silica, as illustrated in Fig. 4. Phosphate also increases down to 70m in concert with Zn and Si, and the slope of the Zn-PO_4 correlation is about 3mmol mol^{-1}. Given this high Zn/PO_4 ratio, one that is within the range measured for oceanic diatoms [40] and higher than the ratio measured in any other type of oceanic phytoplankton to date [40], and given that diatoms are the most important phytoplankton group during the dominant spring bloom in the Black Sea [e.g. 59,60], it seems likely that the photic zone drop in Zn concentrations is dominantly driven by diatom uptake. It is significant, therefore, that this drop in Zn concentrations is associated with no change in Zn isotopes, as further illustrated by the flat trend defined by the blue surface data in Fig. 6a, consistent with the finding that Zn isotopes do not change across a close to two-order-of-magnitude drop in dissolved Zn concentrations driven by diatom uptake in the South Atlantic [17,41]. If this conclusion continues to hold, it is at odds with findings from culture studies [e.g. 22,23]. For example, applying fractionation factors for uptake of Zn into diatom cells found in culture [22], residual surface water $\delta^{66}Zn$ should be driven to values that are +0.4‰ ($\Delta_{cell\text{-}external} = \delta^{66}Zn_{cell} - \delta^{66}Zn_{medium}$ = -0.2‰, high affinity uptake) or +1.6‰ ($\Delta_{cell\text{-}external}$ = -0.8‰, low affinity uptake) across the drop in Zn concentrations seen in the oxic zone of the Black Sea. Though it is theoretically possible that the constancy of the isotopic composition of the residual dissolved pool (in both the Southern Ocean and the Black Sea) could reflect a balance between removal of the light isotope by cellular uptake and the heavy isotope by scavenging [e.g. 23], this would be quite a remarkable coincidence. It is also theoretically possible that the data array in Fig. 6a could be due to a two-step process, whereby Zn is stripped out of the surface layer early in the summer by uptake, potentially *with* an isotopic fractionation, and that this signal is then over-printed by upward mixing of Zn from beneath the photic zone at some time between biological stripping and our sample collection. However, the data array in Fig. 6a would remain flat and linear only if the pre-mixing drawdown brought Zn concentrations to levels in the 10s of pM.

In terms of the overall Zn isotopic balance of the Black Sea oxic layer, the impact of the very light isotopic composition of the Danube input (Table 1) is obviously key. Given that the only output from the surface oxic layer apparently involves no isotopic fractionation, the $\delta^{66}Zn$ of the dissolved pool must simply represent a mixture of Zn from the inputs. The water discharge from the Danube is 191 km^3 yr^{-1} [61], which, with a Zn concentration of 10.5-11 nmol kg^{-1} (Table 1), implies a Zn input of 2.2×10^6 mol yr^{-1} at an isotope composition of -0.8‰. The other known source is the deep basin via water exchange. Taking the Zn concentration and isotope composition of the deep basin to be 0.4 nmol kg^{-1} and +1.1‰, respectively, the turnover time for water between the oxic layer and the deep basin would have to be on the order of 90 years. Given the uncertainties in this calculation, this result may not be significantly different from other estimates of the water turnover time of 100-200 years [e.g. 62]. In any case there are a number of additional considerations. For example, the required deep-surface turnover time is lengthened if the other rivers draining into the Black Sea (about a further 100 km^3 yr^{-1} [61]) collectively have an isotopic composition more like other world rivers, as opposed to the extremely light value of the Danube, or if there are significant non-riverine sources. Alternatively, the water replacement time of the surface layer by the Danube inflow is on the order of 150 years. If the Zn abundance and isotopic composition of the Danube are due to pollution in the lower reaches, it is likely that they have changed over this timescale. Finally, it is possible that this particular sample is contaminated by local pollution. A previous measurement of the Zn concentration of the Danube, on a sample collected right at the outlet to the Black Sea [61], yielded a Zn concentration of 6 nmol kg^{-1}, which, combined with the isotopic composition measured here, would allow a water exchange time of 150 years.

Zn and its isotopes in the euxinic deep water column

As illustrated in Fig. 4, the sharp reduction in Zn concentrations beneath 70m involves a different process from the decrease towards the surface that occurs in step with Si. It is also apparent from the depth profiles in Fig. 3 that the sharp removal of Zn across the redoxcline in the Black Sea is associated with a shift to heavier dissolved Zn isotopes by about 0.9-1‰. As illustrated in Fig. 6a (black points), the pattern across the redoxcline, drawing Zn concentrations down to about 30% of those at the water column maximum, are consistent with a Rayleigh fractionation model involving irreversible preferential removal of the light isotope of Zn by about 0.7‰ (grey arrow, α = 0.9993, see caption for details of the calculation). Landing and Lewis

[67] present a modelling analysis of the equilibrium speciation of a number of metals in the Black Sea water column and conclude that the dominant inorganic dissolved species of Zn in the sulphidic zone is $ZnS(HS)^-$, as opposed to a mixture of Zn^{2+} (major), $ZnCl^+$ and $ZnCO_3^0$ (both minor) in the upper oxic zone. Fujii et al. [69] used *ab initio* methods to calculate the magnitude of Zn isotope fractionation between different dissolved species of Zn. These calculations suggest $\Delta^{66}Zn_{Zn2+-ZnS(HS)-} = +0.73‰$ at 25°C. If the mix of species in the oxic Black Sea pool includes the minor amounts of carbonate and chloride complexes suggested by Landing and Lewis [67], the Δ value between the oxidised pool of Zn and the sulphidic pool is +0.64‰. Thus, the pattern across the redoxcline is consistent with a shift in Zn speciation to sulphide species, partitioning of the light isotopes into these species, and their partial removal from the dissolved pool. Apart from the fact that nothing more complex than a simple Rayleigh model is required by the data, there are also reasons to suspect that, once Zn is sulphidised, back equilibration with the non-sulphidised pool stops. Daskalakis and Helz [68] note that the Black Sea water column may be close to saturation with respect to sphalerite (ZnS) at the redoxcline. On the other hand, the sulphidised species of Zn may be less stable in solution against scavenging.

The data in Fig. 6a from beneath about 130m (orange) depart from the grey arrow defined by an α of 0.9993, and suggest further removal of Zn from the dissolved pool, such that deep Zn concentrations ultimately reach about 5% of the water column maximum, with little further isotopic fractionation. In the model calculations of Landing and Lewis [67] and Daskalakis and Helz [68], sulphidised species of Zn are found to be dominant at dissolved sulphide levels equivalent to around 130m and below, versus a negligible pool of residual oxidised Zn. Thus, the driver for the shift to heavy isotopes is removed at this point. It is likely, however, that the dissolved sulphide species will continue to be slowly scavenged/removed to mineral phases. Thus the orange data for the deep water column on Fig. 6a is completely consistent with continued slow removal of Zn without significant isotopic fractionation associated with the removal process itself.

The ultimate fate of the sulphidised and scavenged water column Zn is the euxinic sediments of the deep Black Sea, and the sediment data presented here provide further support for the scenario outlined above. As noted earlier, the sediment data in Fig. 5 imply an authigenic $\delta^{66}Zn$ around +0.5 to +0.6‰. Firstly, this is about 0.6‰ lighter than the deep Black Sea water column, suggesting that the equilibrium isotopic fractionation between the oxic and sulphidised pool of Zn calculated by *ab initio* methods [69] is sufficient of itself to explain the sediment-dissolved isotopic difference. Secondly, given the drop in Zn concentrations from the surface to the deep basin of factor 20 or so, the ultimate fate of the vast majority of the Zn that is fed into the Black Sea must be the sediment. The overall budget of Zn isotopes in the Black Sea is complicated by the potential influence of the Danube apparent in the surface, though the measured light isotope composition and high concentration may be anthropogenic in origin. Such a budget would also require data for the Zn concentration and isotopic composition of the deep input, as noted above. It is, nonetheless, intriguing that the $\delta^{66}Zn$ of authigenic sedimentary Zn is very close to the value seen almost everywhere in the deep open ocean. Indeed, the behaviour of Zn in the Black Sea water column and sediments is reminiscent of that of Mo, for which euxinic sediments also record a $\delta^{98}Mo$ value very close to the open ocean due to near quantitative removal in the sulphidic deep basin [e.g. 70-72].

Processes controlling Ni and its isotopes in the water column

The behaviour of Ni and its isotopes shows similarities to that of Zn, as well as some very important differences. One such difference is that variations in Ni concentrations in the water column are subdued, at only ±15% versus the factor 20 or so seen for Zn. Despite this, variation in the isotopic composition of Ni is very substantial, at about 1.5‰, requiring very large isotope effects associated with the sources and sinks of Ni to the Black Sea water column.

Nickel concentrations and isotopic compositions are anti-correlated over the upper 300m of the water column (Fig. 3), an observation that is confirmed by Fig. 6b. The implication of Fig. 6b, at least for data in the upper 300m of the water column, is that variations in the concentration of Ni are associated with an isotope fractionation of about 4‰ (grey arrow in Fig. 6b), which is very large in the context of intermediate mass metal isotope systems. As mentioned earlier with respect to Zn, it is well known that intense cycling of

Mn occurs across the Black Sea redoxcline [e.g. 57, 63-65], with soluble reduced Mn diffusing up from the suboxic/sulphidic portion of the water column into the oxic layer where it precipitates as Mn oxide particulates that sink back into the sulphidic zone. As noted by many authors [e.g. 37,73], Ni has a great affinity for Mn oxide surfaces, via both sorption and structural incorporation, and Ni concentration variations from 0-600 nM in pore waters of reducing sediments are completely controlled by Mn redox chemistry [74]. The details of water column profiles either side of the redoxcline of the Black Sea clearly indicate the greater importance of Mn redox chemistry for Ni relative to Zn, with a prominent maximum in dissolved Ni coinciding with a peak in dissolved Mn [e.g. 57]. In our data, this Ni maximum is associated with a prominent minimum in isotopic compositions, and it is this anti-correlation that is primarily driving the very large fractionation implied by the data array for the upper 300m in Fig. 6b. Measurements of Ni isotopes in Fe-Mn crusts ([37], see Fig. 1) do not record the large isotopic effects required to explain the data in Fig. 6b. However, experiments that have so far only been reported in an abstract [75] suggest that Ni sorption to Mn oxide from synthetic seawater is indeed associated with a $\Delta^{60/58}Ni_{sorbed\text{-}dissolved} = -4‰$, though the mechanism for this large isotope effect is not yet clear.

Beneath 300m, Ni data exhibit a very different pattern, as highlighted by the orange data on Fig. 6b, suggesting a different controlling process. In this case, the spread in concentrations is too small to clearly identify any fractionation associated with the variation in concentration, but the data are at least consistent with a process that is likely to be occurring in the deep Black Sea. Landing and Lewis [67] also modeled the equilibrium speciation of Ni in the Black Sea water column and, as for Zn, concluded that the dominant inorganic dissolved species in the sulphidic zone is $NiS(HS)^-$, again as opposed to a mixture of Ni^{2+} (major), $NiCl^+$ and $NiCO_3^0$ (both minor) in the upper oxic zone. Again as for Zn, Fujii et al. [76] used *ab initio* methods to calculate the magnitude of Ni isotope fractionation between different dissolved species of Ni. Though the Ni sulphide complex identified by Landing and Lewis [67] was not specifically modelled by Fujii et al. [76], they do find $\Delta^{60}Ni_{Ni2+\text{-}Ni(HS)+} = +0.66‰$ at 25°C. Such a fractionation is at least consistent with the data array beneath 300m in the water column of the Black Sea, with the exception of a single datapoint (Fig. 6b).

As noted by Little et al. [48], one initially puzzling aspect of Black Sea sediment data for Ni is that euxinic sediments *are* significantly enriched despite the fact that deep Ni concentrations are not significantly lower than at the surface. The solution for this conundrum suggested by these authors is that there is significant addition of Ni to the deep Black Sea via a benthic Fe/Mn redox shuttle. The transport of Fe and Mn from the shelf to the open basin may occur via nano-particulate oxides [53], which will carry sorbed trace metals. This suggestion is supported by the presence of a fine particle layer that forms on the shelf via reoxidation of sediment-derived reduced dissolved Mn and Fe and spreads laterally throughout the Black Sea. This layer is rich in Mn, Fe and other trace metals (including particulate Ni, Cu, and Zn; [57]). In this scenario, the relative homogeneity of water column Ni concentrations would imply that removal to sediment of sulphidised species, either by scavenging or incorporation into pyrite, keeps pace with supply of Ni from the margins via delivery of Mn oxide particulates and their solubilisation in the deep water column. The isotope composition measured for the Danube here (+1.25‰, Table 3) and the homogeneous isotope composition of the open ocean that is likely to feed the deep Black Sea via inflow through the Bosphorous (about +1.44‰), with the addition of a small amount of light Ni via the particulate shuttle, suggests that the overall input of Ni to the Black Sea is likely to have a $\delta^{60}Ni$ somewhat lighter than +1.35‰, with the balance between these dissolved and particulate sources determining exactly how much lighter. The $\delta^{60}Ni$ of euxinic Black Sea sediments is around +0.3 to +0.6 (Fig. 5b). Given the fractionation into sulphide species of 0.7‰, and if removal as a sulphidised species represents the final pathway for transfer to sediment, this would suggest an overall input somewhere between +1.0 and +1.3‰, qualitatively consistent with all the above.

Implications for the oceanic budgets of Zn and Ni isotopes

Zinc and Ni concentrations and isotopes, despite being controlled by rather similar redox-related processes, exhibit contrasting features in the Black Sea because of differences in their partitioning between dissolved and particulate phases. The near quantitative removal of Zn in the deep sulphidic water column drives the dissolved load to very heavy isotopic compositions because the latter represents a small residual pool. The

zinc supply to the deep Black Sea must represent a mixture of surface water Zn, with [Zn] < 1 nM, $\delta^{66}Zn$ = +0.2 to +0.3‰, and Zn derived from the open ocean via the Mediterranean, likely to have 5-10 times more Zn and $\delta^{66}Zn$ ~ +0.5‰. Thus the authigenic pool in the sediment probably gets close to recording the isotopic composition of Zn that is fed into the deep Black Sea from outside. In this sense the behaviour of Zn in the Black Sea is analogous to Mo [e.g. 70-72]. Authigenic Ni in sediment, on the other hand, is isotopically quite different from the inputs to the deep basin due to removal that is very far from quantitative. Ni is also complicated by its affinity for Mn oxides, and the cycling of Ni sorbed to Mn between the oxidised and reduced portions of the Black Sea system. In both cases, however, the differences between the deep water column and the sediment come close to quantifying the isotope fractionation during sulphidisation and sequestration to particulates, and in both cases there is significant preferential removal of the light isotope to sediment. The magnitude of these isotope effects are consistent with those found by *ab initio* calculations of equilibrium fractionation factors between metal species present in oxic versus sulphidic environments [69,76], though for Ni *ab initio* calculations have not yet been performed for the precise sulphide species identified by Landing and Lewis [67] in the water column of the deep Black Sea.

We argue that a process similar to that we have identified in the Black Sea is likely to have important consequences for the marine budget of Zn and Ni. The rate at which seawater is processed through the Black Sea is far too slow for this basin itself to be quantitatively important for whole ocean Ni and Zn budgets. However, and as noted in the introduction, the ocean-facing upwelling margin of the Americas is floored by sediment that is enriched in Zn that is isotopically light [38]. As also noted in the introduction, it seems increasingly unlikely that the light Zn is delivered to the sediment by photosynthetic uptake. Using the Zn data presented in this paper, we have been able to separate the impact of biological uptake from that of inorganic speciation changes, and the data for the photic zone again show that uptake into cells is associated with no isotopic effect. We suggest, therefore, that while the delivery of Zn to open ocean organic-rich sediments requires uptake into cells in the photic zone, the generation of the isotopically light signature of authigenic Zn does not occur there. Instead, we suggest that it is likely to happen via the release of isotopically unfractionated cellular Zn into pore waters and the preferential sequestration of light isotopes into the sulphide phases. In the Black Sea this process starts within the water column, via the stabilisation of dissolved sulphide species. Some authors [e.g. 16,18,78] have suggested that metals may be precipitated in sulphides in euxinic microenvironments around sinking biological particles, and that this process could explain the homogeneously heavy deep ocean [16,18]. We tentatively suggest instead that, in the open ocean, the process is more likely to occur within sediment, which at upwelling margins become sulphidic a few cm beneath the sediment-water interface.

A requirement of this scenario is that light Zn and Ni are non-quantitatively incorporated into sedimentary sulphide, and that residual, relatively heavy Zn and Ni, is released back to the dissolved phase from pore waters. A quantitative assessment of the importance of such a process must await the acquisition of data for pore waters and different components of the sediment from upwelling margins, something that we currently have under way. It is, however, possible to put forward a plausible qualitative scenario. For example, it is well known that bottom water at upwelling margins is anoxic or close to anoxic, whereas pore waters often become sulphidic at depths of a few cm, if not at the sediment-water interface (e.g. as summarized in [38,80]). Thus sulphide is available for the fixation of Zn and Ni that is released from the microbial respiration of organic matter, including by aerobic respiration just above the sulphidic zone. This process is very unlikely to be quantitative, however. Heavy aqueous phase Zn and Ni that is not sequestered into sulphide phases is likely to be lost back to the water column, either by diffusion down the concentration gradient away from the respiration-fuelled source near the top of the sediment, or simply by re-suspension of the top few cm of the sediment-porewater package. Though published pore water Zn concentrations are very scarce, we note that precisely this scenario has been put forward to explain pore water Zn concentrations in anoxic lake sediments [81, see their Fig. 10].

The view of the oceanic Zn isotopic cycle that we advocate here is summarised in Fig. 7, modified after that in Little et al. [77]. We suggest that the Zn pool entering the oceans via rivers, dust and possibly hydrothermal and benthic sources is isotopically split within the oceans into two pools. Nearly all the Zn in the open ocean is organically complexed, so that this pool would be close to the oceanic average $\delta^{66}Zn$, of

around +0.5‰. The minor Zn^{2+} pool will be isotopically lighter [79]. This free Zn^{2+} pool is scavenged to Fe-Mn oxide particulates in the open ocean, favouring the heavy isotopes as evidenced by both observations and experiments [32,66]. This heavy sink is augmented by equally heavy, but smaller, outputs to siliceous and carbonate sediments [32]. The heavy output is balanced by the removal of isotopically light Zn in reducing environments, and we note that the maximum Zn isotopic shift seen by Little et al. [38] in organic-rich sediments versus the deep ocean dissolved pool, of about 0.7‰, is the same as predicted by Fujii et al. [69] between oxidised and sulphidised species. We emphasise that this is the maximum isotopic fractionation imprinted on the organic-rich sediments, equivalent to the sequestration of a very small portion of the Zn released from organic matter into sulphide. Most of the data for authigenic Zn in the Little et al. [38] data are heavier than -0.2‰, and imply a minimum fractionation between authigenic and seawater Zn of about 0.3‰. Mass balance in Rayleigh-type model would then require that the fraction of Zn sequestered into sulphide in this environment can be as much as 50% of the pool released from organic matter. Precisely how much Zn is fixed into sulphide versus release back to seawater will be controlled by a number of parameters, such as sedimentation rate, organic-carbon supply, the depth at which sulphide is generated, and the variation in porewater Zn/S ratio with depth as influenced, for example, by the precipitation of FeS in the zone of Fe oxide reduction below the level at which aerobic respiration occurs but which would titrate out a portion of the sulphide diffusing upwards. At this stage we know much less about the Ni budget of the oceans, so that it is too early to draw a similar schematic for Ni as in Fig. 7. But it is clear from Fig. 1 that a light output of Ni is also essential to balance the oceanic cycle, and we suggest that the data presented here for the Black Sea also point towards sulphidisation as the controlling process.

As noted in the introduction, the two studies that have identified a benthic source of Zn have seen locally *light* Zn in bottom waters (Fig. 1; [16,18]). One instance of these light values, on continental margins either side of the North Atlantic involves sediments that are not reducing, such that this finding, while important for the overall input to the oceans and included in Fig. 1, is not necessarily relevant to the ideas put forward in this paper. On the other hand, Conway and John [18] find a source of light Zn to bottom waters from the anoxic sediments of the San Pedro Basin on the California Margin, while the scenario favoured here requires the return of heavy Zn to the water column in these situations. These authors put forward two options for the light source in the San Pedro Basin: release of biogenic Zn or dissolution of sulphides remobilised as colloids as the deep basin is periodically flushed with higher oxygen water. As noted above, the future resolution of the Zn budget of the oceans will depend on further studies in this type of setting, including porewater analyses and with the aid of benthic chambers, in order to deconvolve the relative impact of this (so far single) observation from the San Pedro versus the predictions made here.

Concluding Remarks

The emphasis in this contribution on the importance of sulphidic environments for the oceanic budgets of Zn and Ni suggests parallels with the isotopic systems of other elements like Mo [e.g. 70-72]. In many respects, the basic processes controlling the oceanic budgets of all these elements are the same, but with a spectrum of behaviours generated by differences between the quantitative importance of different aspects of these basic processes. Euxinic sediments are important sinks for Mo, as they are suggested to be here for Zn and Ni. The stepwise sulphidisation of oxidised molybdate (MoO_4^{2-}) to tetrathiomolybdate (MoS_4^{2-}) is also associated with (large) isotope fractionations [81], with the sulphidised species of Mo being isotopically light, as for Zn and Ni. For Mo, the near quantitative conversion of molybdate to tetrathiomolybdate, coupled to removal of the latter to sediment, results in burial of Mo in the euxinic sediments of the Black Sea that is isotopically very close to the open ocean source, at δ^{98}Mo around +2.3‰. In terms of mass balance, this is at the other end of the spectrum from Ni. The rate at which Ni is sulphidised and removed to euxinic sediment is slow compared to the rate at which it is supplied to the deep Black Sea water column, so that only a small fraction of the Ni transiting the deep basin is sulphidised and transferred to sediment. The result is a large isotopic difference between the sources of Ni to the deep Black Sea on the one hand - open ocean water at depth through the Bosphorous modified by the Danube inflow at the surface and transfer of particulate Mn-oxide associated Ni from the margins – and authigenic Ni in the sediment on the other hand. The behaviour of Zn is closer to Mo: near quantitative removal from the deep basin to sediment, authigenic isotopes that are similar to the inputs, and a residual water column pool that is very small and isotopically fractionated relative to the source (this study, for Mo see [72]). A complication with the application of Mo isotopes to

understanding the balance between oxic conditions versus euxinia in the past oceans is that light isotopes are sequestered into both the oxic sink *and* into sulphidic species [70-72, 82]. In the Black Sea the euxinic sink removes Mo quantitatively so that the fractionation associated with sulphidisation is not expressed. However, studies in Earth history are actually dominated by situations where this is not the case [e.g. 28,83,84], leading to some uncertainty in the precise meaning of secular changes in the Mo isotopic composition of the oceans. The intriguing aspect of the view of the Zn isotopic cycle put forward in the present study is that the isotopic effects of oxic versus euxinic sinks are opposite in sign, suggesting intriguing potential for the application of Zn isotopes in parallel with systems like Mo in Earth history.

Acknowledgements

This research was supported by ETH Zürich, Swiss SNF grant "Understanding the oceanic cycling of trace metal micronutrients" (200021_153087/1) and NERC grant "Nickel isotopes as tracers of modern and ancient biogeochemical processes" (NE/F019092/1) to D.V. and by the Netherlands Organisation for Scientific Research (NWO, www.nwo.nl/en) as part of GEOTRACES under project number 822.01.015. **We** are grateful to Jan van Ooijen and Sharyn Ossebaar for measurement of dissolved sulphide and silicate, and to Lesley Salt and Nikki Clargo for dissolved oxygen measurements. We are very grateful to Laura Wasylenki and two anonymous reviewers for comments on an earlier version of this paper that greatly improved its clarity, and to Maeve Lohan for editorial handling.

Data accessibility: all the new data for this study are included in tables in the paper.

Competing interests: none of the authors have any competing financial interests.

Author contributions: MBA and MJAR collected the Black Sea water column samples. TWL provided the Black Sea sediment samples. SHL, CA, and VC did the isotopic analyses. DV conceived, designed and coordinated the study and drafted the manuscript. All authors read and commented on the draft, and gave final approval for publication.

References

1. Bruland, K.W. 1980 Oceanographic distributions of cadmium, zinc, nickel, and copper in the North Pacific. *Earth Planet. Sci. Lett.* **47**, 176-198.

2. Martin, J.H. 1990 Glacial-interglacial CO_2 change: the iron hypothesis. *Paleoceanography* **5**, 1-13.

3. Bermin, J., Vance, D., Archer, C. & Statham, P.J. 2006 The determination of the isotopic composition of Cu and Zn in seawater. *Chem. Geol.* **226**, 280-297.

4. Boyle, E.A. & 20 others 2012 Geotraces IC1 (BATS) contamination-prone trace element isotopes Cd, Fe, Pb, Zn, Cu and Mo intercalibration. *Limnol. Oceanogr. Methods* **10**, 653-665.

5. Takano, S., Tanimazu, M., Hirata, T. & Sohrin, Y. 2013 Determination of isotopic composition of dissolved copper in seawater by multi-collector inductively-coupled plasma mass spectrometry after preconcentration using an ethylenediaminetriacetic acid chelating resin. *Anal. Chim. Acta* **784**, 22-41.

6. Conway, T.M., Rosenberg, A.D., Adkins, J.F. & John, S.G. 2013 A new method for precise determination of iron, zinc and cadmium stable isotopes ratios in seawater by double-spike mass spectrometry. *Anal. Chim. Acta* **793**, 44-52.

7. Vance, D., Archer, C., Bermin, J., Perkins, J., Statham, P.J., Loham, M.C., Ellwood, M.J. & Mills, R.A. 2008 The copper isotope geochemistry of rivers and the oceans. *Earth Planet. Sci. Lett.* **274**, 204-213.

8. Thompson, C.M. & Ellwood, M.J. 2014 Dissolved copper isotope biogeochemistry in the Tasman Sea, SW Pacific Ocean. *Mar. Chem.* **165**, 1-9.

9. Takano, S., Tanimazu, M., Hirata, T. & Sohrin, Y. 2014 Isotopic constraints on biogeochemical cycling of copper in the ocean. *Nature Comms.* **5**, 5663, doi: 10.1038/ncomms6663.

10. Radic, A., Lacan, F. & Murray, J.W. 2011 Iron isotopes in the seawater of the equatorial Pacific Ocean: new constraints for the oceanic cycle. *Earth Planet. Sci. Lett.* **306**, 1-10.

11. Conway, T.M. & John, S.G. 2014 Quantification of dissolved iron sources to the North Atlantic Ocean. *Nature* **511**, 212-215.

12. Abouchami, W., Galer, S.J.G., de Baar, S.J.G., Alderkamp, A.C, Middag, R., Laan, P., Feldmann, H. & Andreae, M.O. 2011 Modulation of the Southern Ocean cadmium isotope signature by ocean circulation and primary productivity. *Earth Planet. Sci. Lett.* **305**, 83-91.

13. Abouchami, W., Galer, S.J.G., de Baar, S.J.G., Middag, R., Vance, D., Zhao, Y., Klunder, M., Mezger, K., Feldmann, H. & Andreae, M.O. 2011 Biogeochemical cycling of cadmium isotopes in the Southern Ocean along the zero meridian. *Geochim. Cosmochim. Acta* **127**, 348-367.

14. Xue. Z., Rehkamper, M., Horner, T.J., Abouchami, W., Middag, R., van der Flierdt, T. & de Baar, H.J.W. 2013 Cadmium isotope variations in the Southern Ocean. *Earth Planet. Sci. Lett.* **382**, 161-172.

15. Conway, T.M. & John, S.G. 2015 Biogeochemical cycling of cadmium isotopes along a high-resolution section through the North Atlantic Ocean. *Geochim. Cosmochim. Acta* **148**, 269-281.

16. Conway, T.M. & John, S.G. 2015 The cycling of iron, zinc and cadmium in the North East Pacific Ocean – insights from stable isotopes. *Geochim. Cosmochim. Acta* **164**, 262-283.

17. Zhao, Y., Vance, D., Abouchami, W. & de Baar, H.J.W. 2014 Biogeochemical cycling of Zn and its isotopes in the Southern Ocean. *Geochim. Cosmochim. Acta* **125**, 653-672.

18. Conway, T.M. & John, S.G. 2014 The biogeochemical cycling of zinc and zinc isotopes in the North Atlantic Ocean. *Global Biogeochem. Cycles* **28**, 1111-1128.

19. Cameron, V. & Vance, D. 2014 Heavy nickel isotope compositions in rivers and the oceans. *Geochim. Cosmochim. Acta* **128**, 195-211.

20. Moore, C.M. & 22 others 2013 Processes and patterns of oceanic nutrient limitation. *Nature Geosci.* **6**, 701-710.

21. Lacan, F., Francois, R., Ji, Y. & Sherrell, R.M. 2006 Cadmium isotopic composition in the ocean. *Geochim. Cosmochim. Acta* **70**, 5104-5108.

22. John, S.G., Geis, R.W., Saito, M.A. & Boyle, E.A. 2007 Zn isotope fractionation during high-affinity and low-affinity transport by a marine diatom *Thalassiosira oceanica*. *Limnol. Oceanogr.* **52**, 2710-2714.

23. John, S.G. & Conway, T.M. 2014 A role for scavenging in the marine biogeochemical cycling of zinc and zinc isotopes. *Earth Planet. Sci. Lett.* **394**, 159-167.

24. Arnold, G.L., Anbar, A.D., Barling, J. & Lyons, T.W. 2004 Molybdenum isotope evidence for widespread anoxia in mid-Proterozoic oceans. *Science* **304**, 87-89.

25. Pearce, C.R., Cohen, A.S., Coe, A.L. & Burton, K.W. 2008 Molybdenum isotope evidence for global ocean anoxia coupled with perturbations to the carbon cycle during the early Jurassic. *Geology* **36**, 231-234.

26. Andersen, M.B., Romaniello, S., Vance, D., Little, S.H., R. Herdman, R. & Lyons, T.W. 2014 A modern framework for the interpretation of $^{238}U/^{235}U$ in studies of ancient redox. *Earth Planet. Sci. Lett.* **400**, 184-194.

27. Dahl, T.W., Boyle, R.A., Canfield, D.E. Connelly, J.N., Gill, B.N., Lenton, T.M. & Bizarro, M. 2014 Uranium isotopes distinguish two geochemically distinct stages during the later Cambrian SPICE event. *Earth Planet. Sci. Lett.* **401**, 313-326.

28. Chen, X., Ling, H.F., Vance, D., Shields-Zhou, G., Zhi, M., Poulton, S. Och, L., Jiang, S.-Y., Li, D., Cremonese. L. & Archer, C. 2015 Rise to modern levels of oceanic oxygenation co-incided with the Cambrian radiation of animals. *Nature Comms* **6**, 7142, doi:10.1038/ncomms8142.

29. Kendall, B. & 16 others 2015 Uranium and molydenum isotope evidence for an episode of widespread ocean oxygenation during the late Ediacaran Period. *Geochim. Cosmochim. Acta* **156**, 173-193.

30. Kunzmann, M.,Halverson, G.P., Sossi, P.A., Raub, T.D., Payne, J.L. & Kirby, J. 2012 Zn isotope evidence for immediate resumption of primary productivity after Snowball Earth. *Geology* **41**, 27-30.

31. Pons, M.-L., Fujii, T., Rosing, M., Quitté, G., Télouk, P. & Albarède, F. 2013 A Zn isotope perspective on the rise of continents. *Geobiology* **11**, 201-214.

32. Little, S.H., Vance, D., Walker-Broun, C. & Landing, W.M. 2014 The oceanic mass balance of copper and zinc isotopes investigated by analysis of their inputs and outputs to ferromanganese oxide sediments. *Geochim. Cosmochim. Acta* **125**, 673-693.

33. Maréchal, C.N., Nicolas, E., Douchet, C. & Albarède, F. 2000 Abundance of Zn isotopes as a marine biogeochemical tracer. *Geochem. Geophys. Geosys.* **1**, 10.1029/1999GC000029.

34. Dong, S., Weiss, D.J., Strekopytov, S., Kreissig, K., Sun, Y., Baker, A.R. & Formenti, P. 2013 Stable isotope ratio measurements of Cu and Zn in mineral dust (bulk and size fractions) from the Taklimakan Desert and the Sahel and in aerosols from the eastern tropical North Atlantic Ocean. *Talanta* **114**, 103-109.

35. Pichat, S., Douchet, C. & Albarède, F. 2003 Zinc isotope variations in deep-sea carbonates from the eastern equatorial Pacific over the last 175 ka. *Earth Planet. Sci. Lett.* **210**, 167-168.

36. Andersen, M.B., Vance, D., Archer, C., Anderson, R.F., Ellwood, M.J. & Allen, C.S. 2011 The Zn abundance and isotopic composition of diatom frustules, a proxy for Zn availability in ocean surface water. *Earth Planet. Sci. Lett.* **301**, 137-145.

37. Gall, L. 2013 Nickel isotopic compositions of ferromanganese crusts and the constancy of deep ocean inputs and continental weathering effects over the Cenozoic. *Earth Planet. Sci. Lett.* **375**, 148-155.

38. Little, S.H., Vance, D., McManus, J., Severmann, S. 2016 Critical role of continental margin sediments in the oceanic mass balance of Zn and Zn isotopes. *Geology* **44**, 207-210.

39. Armbrust, E.A. 2009 The life of diatoms in the world's oceans. *Nature* **459**, 185-192.

40. Twining, B.S., Baines, S.B., Bozard, J.B., Vogt, S., Walker, E.A. & Nelson, D.M. 2011 Metal quotas in the equatorial Pacific Ocean. *Deep Sea. Res. II* **58**, 325-341.

41. Archer, C., Vance, D. & Lohan, M. 2016. Zinc and nickel isotope systematics in the South Atlantic Ocean. Goldschmidt abstract, Yokohama, http://goldschmidt.info/2016/program.

42. Murray, J.W., Top, Z. & Özsoy, E. 1991 Hydrographic properties and ventilation of the Black Sea. *Deep Sea Res. A*. **38**, S663-S689.

43. Lyons, T. W., 1991 Upper Holocene sediments of the Black Sea: Summary of Leg 4 box cores (1988 Black Sea oceanographic expedition). Black Sea Oceanography (ed. E. Izdar & J.W. Murray), pp. 401-441, NATO ASI Series, Netherlands, Springer.

44. Lyons, T. W. & Berner, R. A. 1992 Carbon-sulfur-iron systematics of the uppermost deep-water sediments of the Black Sea. *Chem. Geol.* **99**, 1–27.

45. Codispoti, L.A., Friederich, G.E., Murray, J.W., & Sakamoto, C.M. 1991 Chemical variability in the Black Sea: implications of continuous vertical profiles that penetrated the oxic/anoxic interface. *Deep-Sea Res.* **38**, S691-S710.

46. Pakhomova, S., Vinogradova, E., Yakushev, E., Zatsepin, A., Shtereva, G., Chasovnikov, V. & Podymov, O. 2013 Interannual variability of the Black Sea Proper oxygen and nutrients regime: the role of climatic and anthropogenic forcing. *Est. Coast. Shelf Sci.* **140**, 134-145.

47. Rijkenberg, M.J.A., de Baar, H.J.W., Bakker, K., Gerringa, L.J.A., Keijzer, E., Laan, M., Laan, P., Middag, R., Ober, S., van Ooijen, J., Ossebaar, S., van Weerlee, E.M. & Smit, M.G. 2015 "PRISTINE", a new high volume sampler for ultraclean sampling of trace metals and isotopes. *Mar. Chem.* **177**, 501–509.

48. Little, S.H., Vance, D., Lyons, T.W., McManus, J. 2015 Controls on trace metal authigenic enrichment in reducing sediments: insights from modern oxygen-deficient settings. *Amer. J. Sci.* **315**, 77-119.

49. Lyons, T.W. 1997 Sulfur isotopic trends and pathways of iron sulfide formation in upper Holocene sediments of the anoxic Black Sea. *Geochim. Cosmochim. Acta* **61**, 3367–3382.

50. Severmann, S., Lyons, T. W., Anbar, A., McManus, J. & Gordon, G. 2008 Modern iron isotope perspective on the benthic iron shuttle and the redox evolution of ancient oceans. Geology 36, 487–490.

51. Algeo, T. & Lyons, T. 2006 Mo–total organic carbon covariation in modern anoxic marine environments: Implications for analysis of paleoredox and paleohydrographic conditions: *Paleoceanography* **21**, PA1016, http://dx.doi.org/10.1029/2004PA001112.

52. Lyons, T.W., Berner, R.A. & Anderson, R.F. 1993 Evidence for large-scale pre-Industrial perturbations of the Black Sea chemocline. *Nature* **365**, 538-540.

53. Lyons, T.W. & Severmann, S. 2006 A critical look at iron paleoredox proxies: new insights from modern euxinic marine basins. *Geochim. Cosmochim. Acta* **70**, 5698-5722.

54. Cameron, V., Vance, D. Archer C. & House, C.H. 2009 Ni stable isotopes: a novel isotope biomarker. *Proc. Natl. Acad. Sci.* **106**, 10944-10948.

55. Sohrin, Y., Urushihara, S., Nakatsuka, S., Kono, T., Higo, E., Minami, T., Norisuye, K. & Umetani, S. 2008. Multielemental determination of GEOTRACES key trace metals in seawater by ICPMS after preconcentration using an ethylenediaminrtriacetic acid chelating resin. *Anal. Chem.* **80**, 6267-6273.

56. Archer C. & Vance, D. 2004 Mass discrimination correction in plasma source mass spectrometry: an example using Cu and Zn isotopes. *J. Anal. Atom. Spectrom.* **19**, 656-665.

57. Tankéré, S.P.C., Muller, F.L.L., Burton, J.D., Statham, P.J., Guieu, C. & Matin, J.-M. 2001 Trace metal distributions in shelf waters of the northwestern Black Sea. *Cont. Shelf. Res.* **21**, 1501-1532.

58. Szynkiewicz, A. & Borrok, D.M. 2016 Isotope variations of dissolved Zn in the Rio Grande watershed, USA: the role of adsorption on Zn isotope composition. *Earth Planet. Sci. Lett.* **433**, 293-302.

59. Krupatkina, D.K., Finenko, Z.Z., Shalapyonok, A.A. 1991 Primary production and size-fractionated structure of the Black Sea phytoplankton in the winter spring period. *Mar. Ecol. Progr. Ser.* **73**, 25-31.

60. Ediger, D., Soydemir, N. & Kideys, A.E. Estimation of phytoplankton biomass using HPLC pigment analysis in the southwestern Black Sea. 2006 *Deep-Sea Res. II* **53**, 1911-1922.

61. Guieu, C., Martin, J.-H., Tankéré, S.P.C., Mousty, F., Trincherini, P, Bazot, M. & Dai, M.H. 1998 On trace metal geochemistry in the Danube River and western Black Sea. *Estuar. Coast. Shelf Sci.* **47**, 471-485.

62. Neretin, L.N., Volkov, I.I., Böttcher, M.E. & Grinenko, V.A. 2001 A sulfur budget for the Black Sea anoxic zone. *Deep-Sea Res. I* **48**, 2569-2593.

63. Konovalov, S., Samodurov, A., Oguz, T. & Ivanov, L. 2004 Parameterization of iron and manganese cycling in the Black Sea suboxic and anoxic environment. *Deep-Sea Res. I* **51**, 2027-2045.

64. Pakhomova, S.V., Rozanov, A.G. & Yakushev, E.V. 2009 Dissolved and particulate forms of iron and manganese in the redox zone of the Black Sea. *Oceanology* **49**, 773-787.

65. Yigiterhan, O., Murray, J.W. & Tugrul, S. 2011 Trace metal composition of suspended particulate matter in the water column of the Black Sea. Mar. *Chem.* **126**, 207-228.

66. Bryan, A.L., Dong, S., Wilkes, E.B. & Wasylenki, L.E. 2015 Zinc isotope fractionation during adsorption to Mn oxyhydroxide at low and high ionic strength. *Geochim. Cosmochim. Acta* **157**, 182-197.

67. Landing, W.M. & Lewis, B.L. 1991 Thermodynamic modelling of trace metal speciation in the Black Sea. In Black Sea Oceanography (ed. E. Izdar & J.W. Murray), pp. 125-160, NATO ASI Series, Netherlands, Springer.

68. Daskalakis, K.D. & Helz, G.R. 1993 The solubility of sphalerite (ZnS) in sulfidic solutions at 25°C and 1 atm pressure. *Geochim. Cosmochim. Acta* **57**, 4923-4932.

69. Fujii, T., Moynier, F., Pons, M.-L. & Albarède, F. 2011 The origin of Zn isotope fractionation in sulphides. *Geochim. Cosmochim. Acta* **75**, 7632-7643.

70. Barling, J., Arnold, G.L. & Anbar, A.D. 2001 Natural mass-dependent variations in the isotopic composition of molybdenum. *Earth Planet. Sci. Lett.* **193**, 447-457.

71. Neubert, N., Nägler, T.F. & Böttcher, M.E. 2008 Sulfidity controls molybdenum isotope fractionation into euxinic sediments: evidence from the Black Sea. *Geology* **36**, 775-778.

72. Nägler, T.F., Neubert, N., Böttcher, M.E., Dellwig, O. & Schnetger, B. 2011 Molybdenum isotope fractionation in pelagic euxinia: evidence from the modern Black and Baltic Seas. *Chem. Geol.* **289**, 1-11.

73. Peacock, C.L. & Sherman, D.M. 2007 Sorption of Ni by birnessite: equilibrium controls on Ni in seawater. *Chem. Geol.* **238**, 94-106.

74. Shaw, T.J., Gieskers, J.M. & Jahnke, R.A. 1990 Early diagenesis in differing depositional enviromnents: the response of transition metals in pore water. *Geochim. Cosmochim. Acta* **54**, 1233-1246.

75. Wasylenki, L.E., Wells, R.M. & Spivak-Birndorf, L.J. 2014 Ni sorption to birnessite drives a surprisingly large fractionation. *American Geophysical Union Abstracts* **1**, 3623.

76. Fujii, T., Moynier, F., Blichert-Toft, J. & Albarède, F. 2014 Density functional theory estimation of isotope fractionation of Fe, Ni, Cu and Zn among species relevant to geochemical and biological environments. *Geochim. Cosmochim. Acta* **140**, 553-576.

77. Little, S.H., Sherman, D.M., Vance, D. & Hein, J.R. 2014 Molecular controls on Cu and Zn isotopic fractionation in Fe-Mn crusts. *Earth Planet. Sci. Lett.* **396**, 213-222.

78. Janssen, D.J. & Cullen, J.T. 2015 Decoupling of zinc and silicic acid in the subarctic northeast Pacific interior. *Mar. Chem.* **177**, 124-133.

79. Jouvin, D., Louvat, P., Juillot, F., Maréachal, C.N. & Benedetti, M.F. 2009 Zinc isotopic fractionation: why organic matter. *Environ. Sci. Technol.* **43**, 5747-5754.

80. Poulson, R.L., McManus, J., Severmann, S. & Berelson, W.M. (2009) Molybdenum behaviour during early diagenesis: insights from Mo isotopes. *Geochem. Geophys. Geosys.* **10**, Q06010, doi:10.1029/2008GC002180.

81. Zhang, H., Davison, E. Miller, S. & Tych, W. (2005) In situ high resolution measurements of fluxes of Ni, Cu, Fe and Mn and concentrations of Zn and Cd in porewaters by DGT. *Geochim. Cosmochim. Acta* **59**, 4181-4192.

82. Tossell, J.A. 2005 Calculating the partitioning of the isotopes of Mo between oxidic and sulphidic species in aqueous solution. *Geochim. Cosmochim. Acta* **69**, 2981-2993.

83. Westermann, S., Vance, D., Cameron, V., Archer, C. & Robinson, S.A. 2014 Heterogeneous oxygenation states in the Atlantic and Tethys oceans during Oceanic Anoxic Event 2. *Earth Planet. Sci. Lett.* **404**, 178-189.

84. Kendall, B. & 16 others 2015 Uranium and molydenum isotope evidence for an episode of widespread ocean oxygenation during the late Ediacaran Period. *Geochim. Cosmochim. Acta* **156**, 173-193.

Table 1: Chemical and Zn-Ni isotope data for the dissolved load of the Black Sea and River Danube

Station	Bottle No.	Depth (m)	Temp (°C)	S	$[PO_4]$ µmol/kg	Silicate µmol/kg	$[O_2]$ µmol/kg	$[HS^-]$ µmol/kg	[Zn][1] nmol/kg	$\delta^{66}Zn$	2σ	[Ni] nmol/kg	$\delta^{60}Ni$	2σ
2	24	9	25.506	18.233	0.00	1.71	235		0.63	0.18	0.06	11.8	1.17	0.06
2	23	24	11.093	18.360	0.01	3.38	336		1.13	0.18	0.06	11.1	1.19	0.06
2	22	39	8.767	18.453	0.02	4.74	299		1.08	0.20	0.06	11.5	1.20	0.06
2	21	45	8.272	18.600	0.07	8.21	257		1.30	0.27	0.06	11.1	1.25	0.06
2	20	69	8.260	20.017	1.31	39.8	13.9		4.95	0.20	0.06	11.4	1.51	0.06
2	19	84	8.459	20.537	1.72	52.6	4.3		2.91	0.53	0.08	10.9	1.44	0.06
2	18	99	8.533	20.859	6.15	63.8			3.05	0.35	0.07		0.75	0.06
2	17	114	8.587	21.085	5.40	72.5		8.5	1.32	1.16	0.06	12.6	0.81	0.06
2	16	129	8.621	21.217	4.99	80.8		16.1	0.65	1.24	0.06	13.0	0.94	0.06
2	15	145	8.654	21.326	4.89	87.3		22.3	0.53	1.26	0.06	12.1	0.93	0.06
2	14	160	8.682	21.417	4.83	92.3		26.1				12.1	1.30	0.06
2	13	174	8.713	21.503	4.78	98.7		34.5	0.33	1.11	0.07	11.4	1.49	0.06
2	12	204	8.752	21.607	4.93	110		46.4	0.28	1.16	0.08	10.4	1.72	0.06
2	11	250	8.802	21.743	5.07	128		70.2	0.26	1.05	0.09	10.3	1.95	0.06
2	10	300	8.836	21.849	5.24	143		93.6	0.26	1.09	0.06	10.3	1.97	0.06
2	9	399	8.872	21.988	5.77	173		143						
2	8	498	8.888	22.087	6.40	204		192	0.30	1.07	0.06	11.3	1.83	0.06
2	7	749	8.918	22.240	7.13	252		289						
2	6	999	8.960	22.306	7.57	278		348	0.28	1.28	0.06	12.2	2.22	0.06
									0.29	***0.97***	***0.06***			
2	5	1249	9.000	22.332	7.78	291		382						
2	4	1499	9.037	22.342	7.98	301		398	***0.48***	***0.70***	***0.06***	11.9	1.81	0.06
2	3	1749	9.079	22.349	8.06	312		419						
2	2	2070	9.116	22.349	7.98	309		422	0.42	1.05	0.06	12.3	1.80	0.06
									0.95	***0.36***	***0.10***			
2	1	2120	9.123	22.349	8.10	313		422	0.44	1.02	0.06	12.2	1.84	0.06
									0.44	***0.84***	***0.06***			

[1]For some samples from Station 2 we analysed a second bottle for Zn and its isotopes, following anomalous results from the analysis of the first bottle. The anomalous results are shown in bold italics while the, normal, results from the second bottle are shown in normal typescript. See results section in main text for further discussion.

Table 1 (continued): Chemical and Zn-Ni isotope data for the dissolved load of the Black Sea and River Danube.

Station	Bottle No.	Depth (m)	Temp (°C)	S	$[PO_4]$ µmol/kg	Silicate µmol/kg	$[O_2]$ µmol/kg	$[HS^-]$ µmol/kg	[Zn] nmol/kg	$\delta^{66}Zn$	2σ	[Ni] nmol/kg	$\delta^{60}Ni$	2σ
5	24	10	22.372	18.124	0.02	2.06	260		0.78	0.23	0.06	11.5	1.20	0.06
5	23	29	9.286	18.257	0.03	3.93	315							
5	22	40	8.415	18.351	0.03	4.80	297		1.10	0.19	0.06	11.1	1.24	0.06
5	21	54	7.663	18.892	0.59	18.9	172							
5	20	69	8.060	19.711	1.21	35.4	48.0							
5	19	84	8.386	20.309	1.20	45.7	10.4							
5	18	100	8.498	20.741	4.31	59.3	0.4		2.85	0.49	0.06	11.8	1.17	0.06
5	17	110	8.552	20.945	6.89	64.1								
5	16	130	8.605	21.144	4.99	74.3		8.4	1.43	1.04	0.06	12.6	0.83	0.06
5	15	145	8.642	21.271	4.75	81.5		14.5						
5	14	149	8.663	21.298	4.76	82.7		15.1	0.75	1.20	0.06	12.3	1.05	0.06
5	13	175	8.702	21.438	4.67	92.6		26.0						
5	12	205	8.782	21.584	4.66	104		37.2	0.47	1.08	0.06	10.4	1.64	0.06
5	11	250	8.811	21.726	4.89	123		63.5						
5	10	300	8.838	21.843	5.22	141		91.1	0.31	1.09	0.06	10.0	2.05	0.06
5	9	400	8.874	21.982	5.68	171		136.5						
5	8	500	8.889	22.081	6.19	198		180.1						
5	7	750	8.918	22.233	7.11	252		265.2	0.32	1.11	0.06	11.6	1.88	0.08
5	6	1000	8.958	22.300	7.53	280		333.3						
5	5	1250	9.000	22.330	7.72	293		374.8	0.33	1.24	0.06	11.7	1.98	0.06
5	4	1500	9.036	22.341	7.82	300		385.5						
5	3	1751	9.079	22.348	7.95	312		402.6						
5	2	1989	9.107	22.349	7.92	314		414.8	0.43	1.09	0.06			
5	1	2040	9.114	22.348	7.99	312		412.6	0.36	1.18	0.06	11.9	1.88	0.06
River Danube														
D1									11.0	-0.80	0.06	18.0	1.27	0.06
D2									10.5	-0.83	0.06	18.1	1.25	0.06

Table 2: Concentration and Zn-Ni isotope data for Black Sea sediments.

Sample	Depth (cm)	[Ni] ppm	[Zn] ppm	[Al] wt. %	Zn/Al ($x10^4$)	Ni/Al ($x10^4$)	$\delta^{66}Zn$	2σ	$\delta^{66}Ni$	2σ
Station 16 (129m, shelf, oxic bottom water)										
16-1	0-2	71	54	5.1	10.6	13.9	0.31	0.09	0.15	0.06
16-2	2-4	93	63	6.4	9.8	14.5	0.25	0.06	0.20	0.06
16-3	4-6	69	50	5.4	9.4	12.8	0.30	0.06	0.19	0.07
16-4	6-8	81	56	5.6	10	14.5	0.28	0.06	0.20	0.06
16-5	10-12	71	53	5.5	9.5	12.8	0.26	0.06	0.21	0.06
16-6	12-14	71	53	5.5	9.7	12.9	0.24	0.06	0.23	0.07
16-7	14-16	74	54	5.7	9.4	13.0	0.23	0.06	0.13	0.06
16-8	16-18	70	47	4.6	10.1	15.2	0.29	0.06	0.34	0.06
Station 16B (160m, shelf, close to chemocline)										
16B-1	0-2	78	86	6.7	13.0	11.7	0.24	0.06	0.19	0.06
16B-2	2-4	90	90	7.0	12.9	12.9	0.37	0.06	0.18	0.06
16B-3	4-6	91	88	6.0	14.6	15.2	0.32	0.06	0.24	0.06
16B-4	6-8	92	77	6.4	12.0	14.4	0.29	0.06	0.20	0.06
16B-5	8-10	93	75	4.5	16.8	21.0	0.36	0.06	0.14	0.06
16B-7	12-14	86	67	4.7	14.2	18.1	0.27	0.06	0.19	0.06
16B-8	14-16	80	70	6.5	10.8	12.3	0.22	0.06	0.14	0.06
16B-9	18-20	65	60	5.8	10.3	11.2	0.32	0.06	0.21	0.06
16B-10	20-22	80	73	6.9	10.6	11.7	0.25	0.06	0.14	0.06
Station 9 (2094m, deep basin, euxinic, Unit I)										
9-1	3-6	45	66	2.5	26.6	18.2	0.49	0.06	0.19	0.06
9-2	8-10	43	44	2.1	20.9	20.5	0.53	0.06	0.23	0.06
9-3	10-12	52	49	2.2	22.6	24.0	0.55	0.06	0.22	0.06
9-4(2)	14-16	21	16	0.7	23.4	30.1	0.52	0.06	0.51	0.06
9-5	16-18	41	32	1.5	21.7	28.1	0.54	0.06	0.21	0.06
9-6	18-20	31	23	1.1	20.7	27.3	0.50	0.06	0.26	0.06
9-7	22-24	35	91	1.1	83.8	31.9	0.52	0.06	0.30	0.06
9-8	24-26	47	26	1.3	20.3	37.1	0.56	0.06	0.23	0.06
Station 14 (2218m, deep basin, euxinic, Unit I)										
14-1	0-2	67	104	4.7	22.2	14.3	0.46	0.06	0.21	0.06
14-2	4-6	54	70	4.1	17.0	13.1	0.47	0.06	0.14	0.06
14-3	8-10	45	45	2.3	19.2	19.1	0.49	0.06	0.25	0.06
14-4	12-14	57	56	3.5	16.0	16.4	0.44	0.06	0.15	0.06
14-5	16-18	70	55	3.3	16.6	21.3			0.19	0.06
14-6	20-22	42	30	1.9	16.3	22.2	0.44	0.06	0.42	0.06

Figure Captions

Figure 1: Summary of our current knowledge of the oceanic cycle of (a) Zn and (b) Ni isotopes. Seawater data [3,4,16-19] given at the top as a range of all measurements for the entire water column (thin horizontal black line) and the average and 1 SD of all data for Ni isotopes, and all data beneath 800m for Zn (thicker portions of horizontal lines and vertical grey bar). Data ranges for the inputs and outputs are shown as thin lines. Where there are sufficient data, the average and 1SD are shown as thicker lines, except for the river data where the thicker portions of the lines show the discharge- and concentration-weighted average isotope composition, thus representing the global dissolved riverine flux to the oceans. Other data sources: rivers [19,32]; dust/aerosol/loess [19, 32-34]; Fe-Mn deposits [32,33,37]; carbonates [35]; siliceous sediments [36]; organic-rich sediments [38]. The range for possible Zn inputs from hydrothermal and benthic sources are taken from the data and discussion in Conway and John [16,18].

Figure 2: Map of the Black Sea showing the stations sampled during leg 2 of the RV Pelagia GEOTRACES cruise, MedBlack (cruise 64PE373, July 2013). Water column stations 2 and 5 studied here are shown as blue circles. Locations of sediment cores discussed in this paper are shown as black squares.

Figure 3: Chemical and Zn-Ni isotopic data for the Black Sea water column. The top panels show an expanded view of the upper 300m, the bottom panels the entire water column. Concentration profiles for sulphide (dashed line in left panels) and oxygen (solid line, left hand panels) are very similar at Stations 2 and 5 and, for clarity, only the Station 5 profiles are shown. Ni and Zn concentrations and isotopic data are shown separately for Stations 2 (filled diamonds) and 5 (open squares).

Figure 4: Zn concentrations versus Si for the upper 70 m of the water column (a, blue, Station 2 plotted as filled diamonds, Station 5 as open squares) and for the entire water column (b). Correlation with Si in the upper oxic photic zone suggests Zn abundances above the concentration maximum at around 70m are controlled by biological uptake. Beneath 70m Si continues to increase while Zn concentrations fall off dramatically.

Figure 5: Zn (a) and Ni (b) isotope data for Black Sea sediments from cores recovered beneath deep water rich in sulphide (filled symbols, Sites 9 and 14), from water depths close to the chemocline (grey-filled symbols, Sites 16B), and from the shelf beneath oxic bottom water (open symbols). Sediments deposited beneath the euxinic water column have Al/Zn ratios up to 5 times lower than oxic sediments, reflecting authigenic enrichment of Zn. The intercept at Al/Zn = 0 of the trend indicated by the grey arrow provides an estimate of the $\delta^{66}Zn$ of this authigenic Zn, at about +0.5 to +0.6‰. Al/Ni ratios in euxinic sediments around a factor of 3 lower than oxic sediments also imply authigenic Ni addition. Though the correlation with Ni isotopes is weaker than for Zn, these data imply a $\delta^{60}Ni$ in authigenic Ni around +0.45±0.15‰.

Figure 6: Zn (a) and Ni (b) concentration and isotopic data for the Black Sea water column in log [concentration] versus delta space. Station 2 shown as filled diamonds, Station 5 as open squares. In the Zn plot, the data at or above the concentration maximum at 70m (blue), where Zn is drawn down towards the surface in the oxic photic zone, removal occurs with little or no fractionation. The grey arrow on the Zn plot shows the modelled evolution of the aqueous phase ($\delta^{66}Zn_{aqeuous}$) as Zn is removed from a starting pool ($\delta^{66}Zn_{starting}$) across the redoxcline with an isotope fractionation factor (α) as shown, with $\delta^{66}Zn_{aqueous} \sim \delta^{66}Zn_{starting} x f^{\alpha -1}$, where f = the fraction of the starting Zn pool remaining. The drawdown of Zn from the dissolved pool (up to about 75%) is associated with an isotope fractionation of about 0.7‰. Beneath about 130m (orange) the dominant process in the Zn data is a further reduction in concentration without much change in isotopic composition. Ni data for the upper 300m can be explained by cycling of Ni between water column and Mn oxide particulates. The data require a very large isotopic effect, of about 4‰ (grey arrow, Rayleigh fractionation model array as for Zn), but this is in agreement with experiments recently reported in abstract form [75]. Data from beneath 300m (orange) lie on a much flatter array, potentially explained by isotope partitioning between sulphidised species that are scavenged and removed and a dissolved pool, consistent with isotope fractionation factors reported in [76].

Figure 7: Summary of the view put forward here of the processes relevant to the overall marine budget of Zn isotopes (modified after Little et al. [77]). The inputs are shown as an arrow on the left. Within the oceans this input is split into two pools (schematic isotopic compositions shown as blue horizontal dashed lines): a dominant ligand-bound pool (ZnL) and a minor free metal ion pool (Zn^{2+}). The ligand-bound pool is shown as heavy relative to the free metal ion [79]. If the oceans are in steady state the isotopic compositions of the outputs (arrows on right) must balance the input. For Zn the outputs to oxic sediments have $\delta^{66}Zn \sim +0.9‰$ [32], consistent with a positive $\Delta_{sorbed\text{-}Zn2+}$ [66]. This is balanced by a light output to organic-rich sediments [48]. It is suggested here that this may be controlled not by delivery of isotopically light Zn to sediment by photic zone uptake, but by preferential sequestration of the light isotopes of Zn to sulphide within sediment.

Vance et al. Figure 1

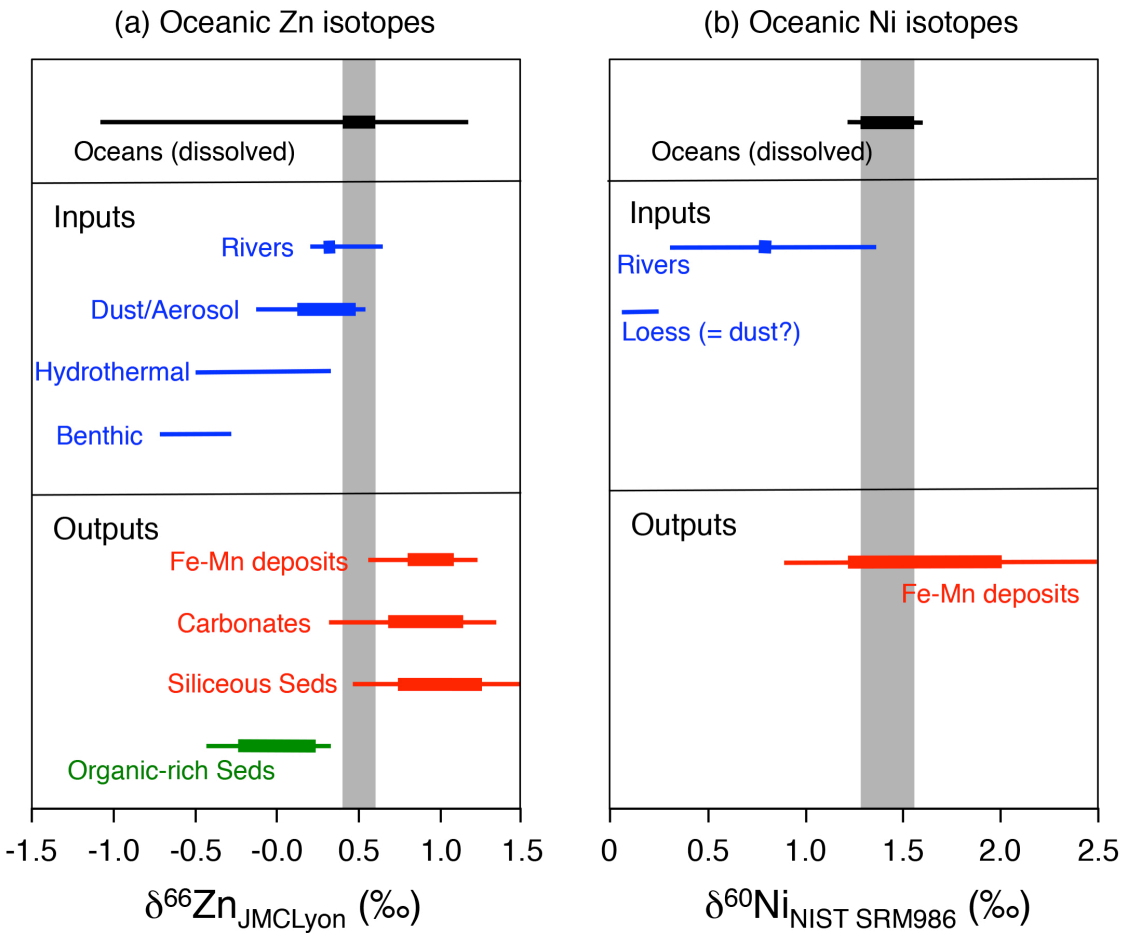

Vance et al. Figure 2

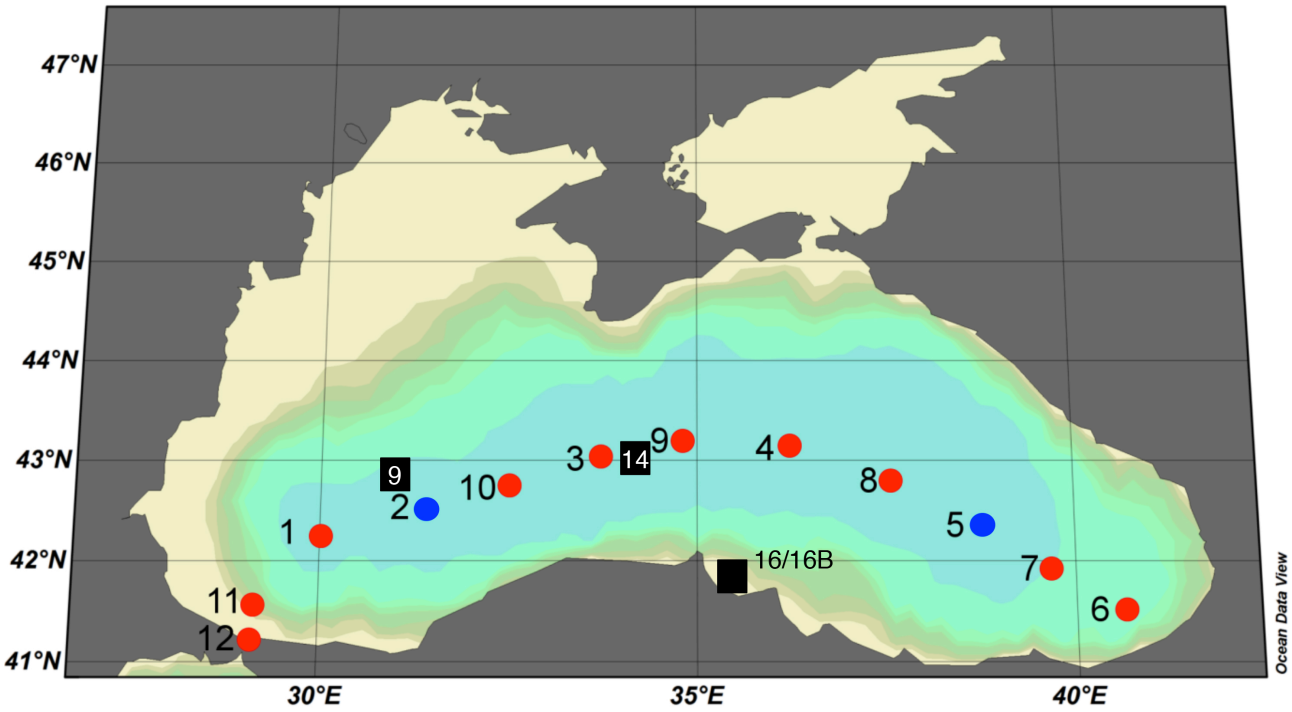

Vance et al. Figure 3

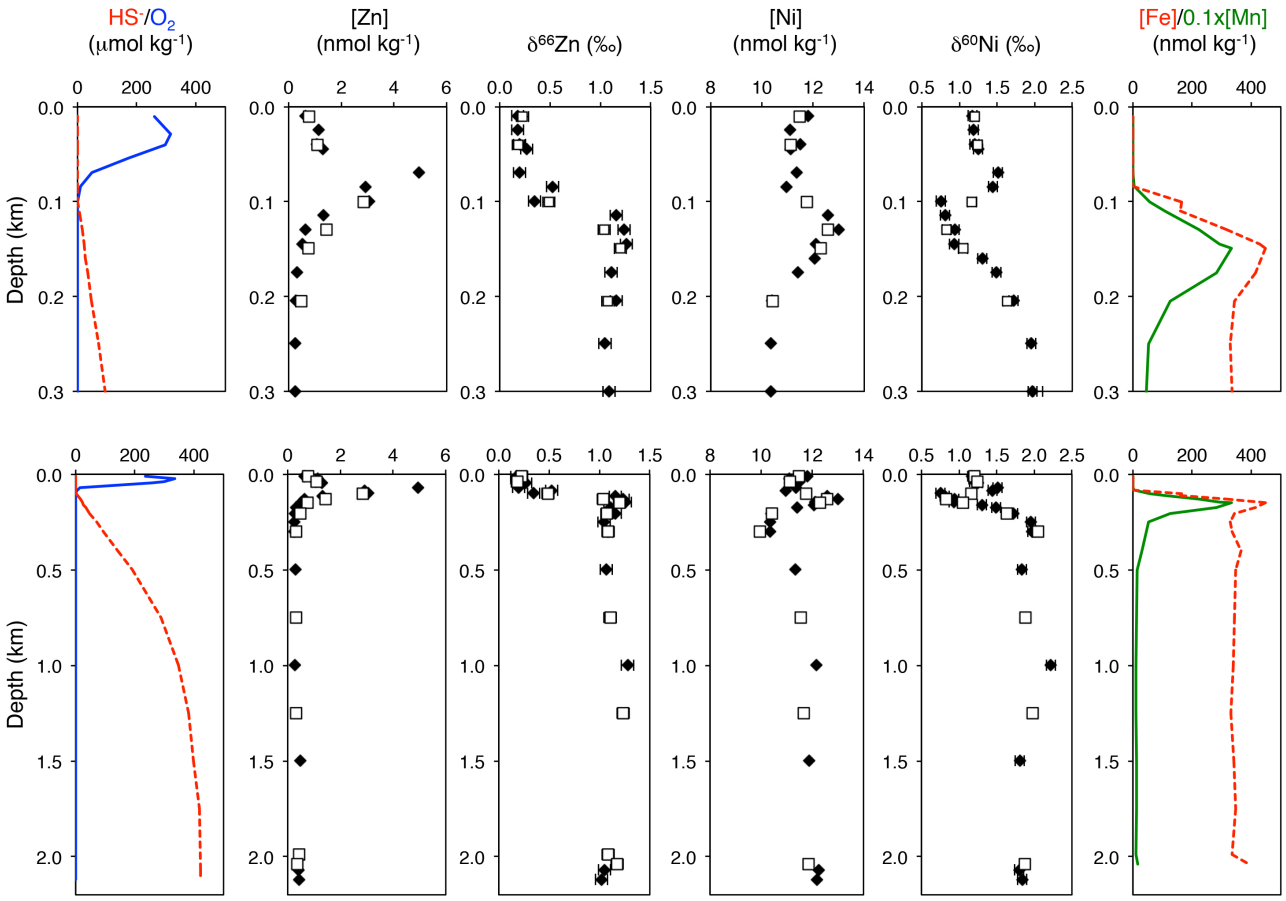

Vance et al. Figure 4

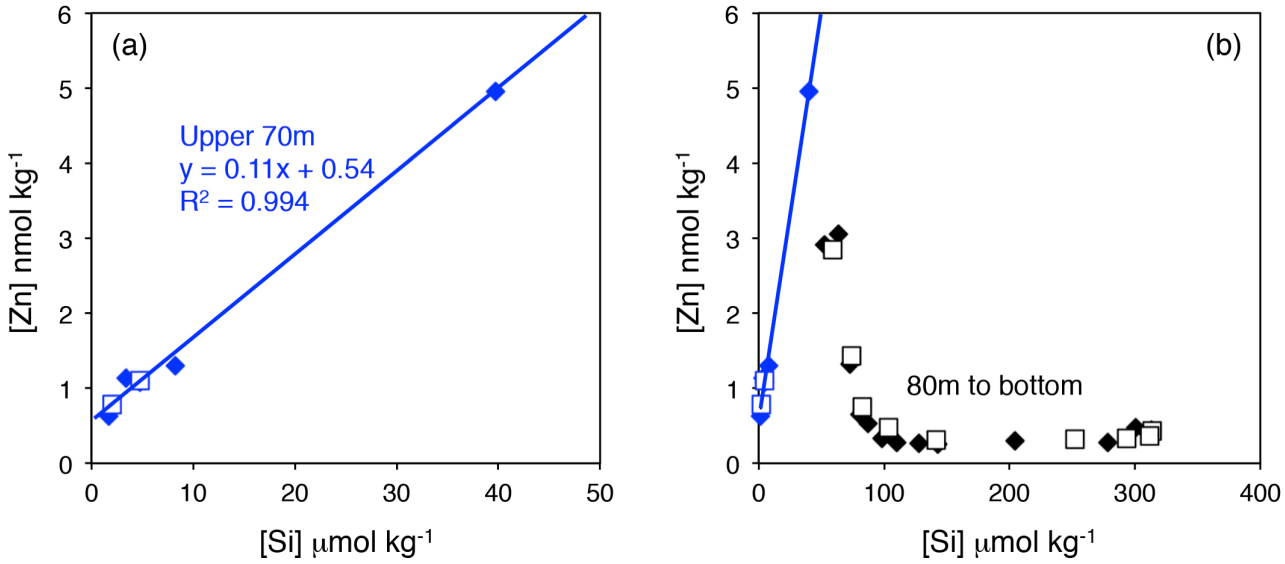

Vance et al. Figure 5

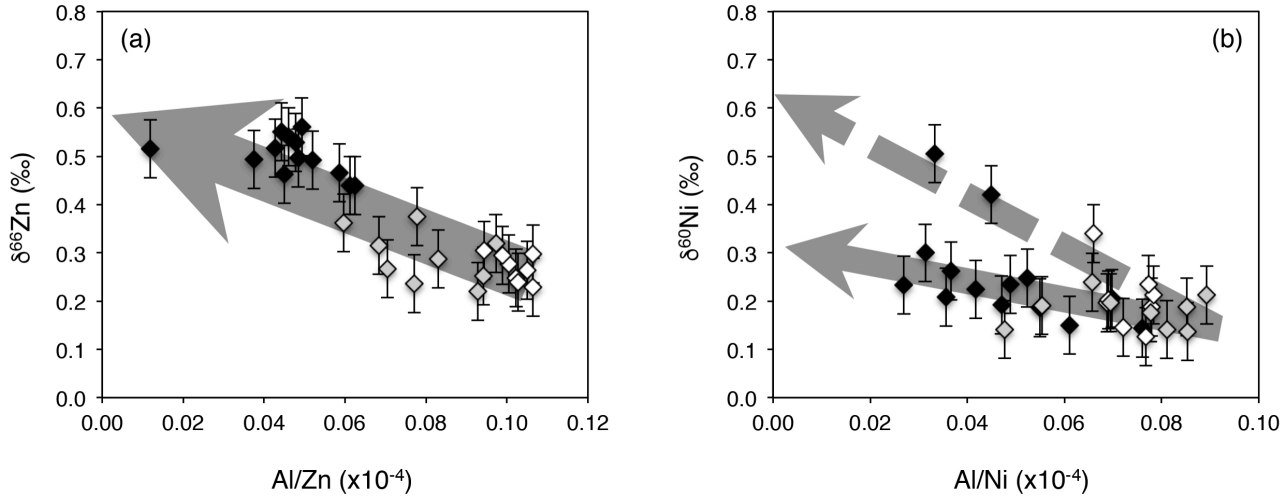

Vance et al. Figure 6

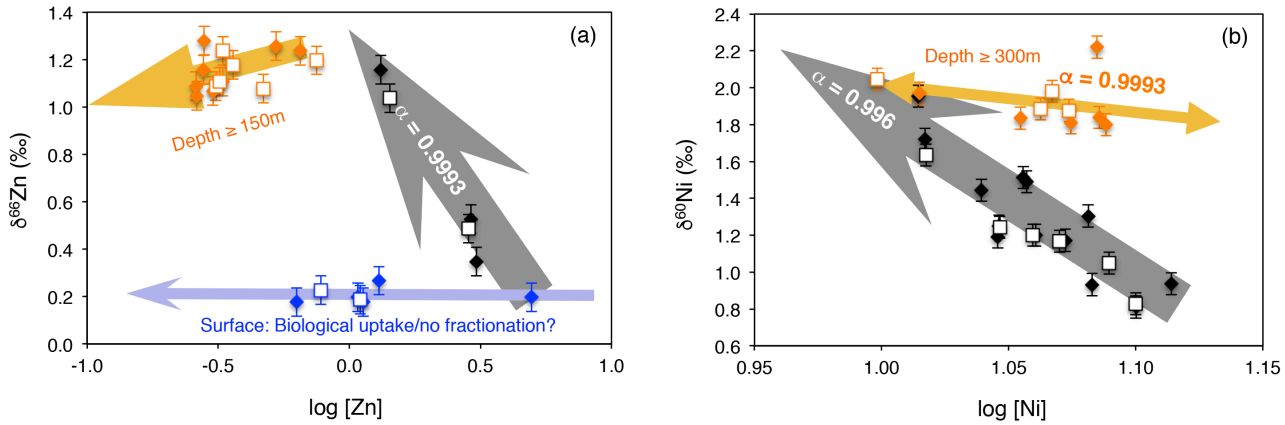

Vance et al. Figure 7